SEARCH FOR NEUTRINO OSCILLATIONS AT LAMPF LOS ALAMOS*

By T. A. Romanowski

The Ohio State University, Columbus**

(Received June 20, 1984)

A method for searches for neutrino masses via the detection of neutrino oscillations is discussed. The experiment in progress at LAMPF meson facility at Los Alamos, E-645, is described.

PACS numbers: 14.60.Gh

Introduction

The postulation of the existence of neutrinos simultaneously generated a question of its mass. There are no fundamental predictions for the neutrino mass and the conventional assumption that it is null is justifiable in view of the existing circumstantial evidence to the contrary.

The Grand Unified Theory (GUTS) of strong, weak and electromagnetic interactions does not distinguish neutrinos from other fermions and there is no special reason why neutrinos should have zero mass. The theoretical estimates for neutrino masses predict it to be small in the range of $(10^{-6}$–$1)$ eV. The mass term for all fermions is constructed by coupling the left-handed and right-handed helicity states which conserve the total lepton number and require that both left and right handed fermions exist. In the case of neutrinos and other neutral fermions a second type of mass term this time lepton number nonconserving can be constructed which is coupled to its own charge conjugate right handed field. This construct can be made without the existence of the right handed neutrinos. In the mass term the lepton number conserving piece is called the Dirac mass term and the lepton violating term the Majorana. In the simplest SU(5) model there are no right handed neutrinos. If the neutrinos which belong to the ordinary weak interactions have a mass then they are in part of Majorana type. The GUTS models can accommodate the right handed neutrinos and support the notion that the neutrino masses at least in part

* Presented at the XXIV Cracow School of Theoretical Physics, Zakopane, June 6–19, 1984.

** Address: High Energy Physics Lab., Ohio State University, 174 W 18-th Av., Columbus OH 43210, USA.

are of the Majorana variety. Neutrino mass terms with significant Majorana terms have as their eigenstates the Majorana neutrinos. The Majorana neutrinos are the CPT eigenstates but within a good approximation they can be treated as CP eigenstates or even as charge conjugation eigenstates. In general the experiments do not differentiate between the Majorana and Dirac neutrinos. The experiment sensitive only to the Majorana terms is that on the no-neutrino double beta decay.

If the neutrinos have mass then the weak or CP eigenstates are not identical with the mass eigenstates. The weak eigenstates would be now a mixture of mass eigenstates characterized by a unitary mixing matrix. The experimental consequences would be as follows:

(1) The decay spectra of mesons and leptons would be altered by dominantly coupled neutrinos.
(2) Existence of secondary mass peaks in the decay spectra produced by finite masses of subdominantly coupled neutrinos.
(3) Unstable neutrinos and neutrino decays.
(4) Neutrino oscillations
(5) Neutrino double beta-decay.

Presently existing "best" limits on the neutrino masses are:

$$m_{\nu_e} > 20 \text{ eV ITEP [1]},$$

$$m_{\nu_\mu} < 490 \text{ keV SIN [2]},$$

$$m_{\nu_\tau} < 164 \text{ MeV SLAC [3]}.$$

There is no firm experimental data which support the existence of neutrino masses. However some experiments infer the neutrino masses or can not exclude such a possibility. The evidence for the possible existence of the neutrino masses will be discussed below. The experiment at ITEP which investigated tritium decay in valine

$$^3\text{H} \rightarrow {}^3\text{He}^+ + e^- + \bar{\nu}_e$$

TABLE I

Future β-decay experiments

Experiment	Source	Resolution (rms)	Sensitivity
Fackler et al. (Rock-FNAL-LLL)	Solid molecular ^{3}H	1–2 eV	$m_\nu > 4$ eV
Boyd (Ohio State)	Solid molecular ^{3}H	10 eV	$m_\nu > 10$ eV
Bowles et al. (LAMPF)	Atomic ^{3}H	40 eV	$m_\nu > 10$ eV
Clark (IBM)	Solid ^{3}H	5 eV	—
Heller et al. (UC Berkeley)	^{3}H in semiconductor	100 eV	$m_\nu > 30$ eV
Graham et al. (Chalk River)	—	10 eV	$m_\nu > \sim 20$ eV
Bergkvist	^{3}H in valine	~ 25 eV	$m_\nu > 19$ eV
Kundig (Zurich)	—	5 eV	$m_\nu > 10$ eV
INS (Japan)	—	13 eV	$m_\nu > 25$ eV

reported a range for the ν_e mass to be 14 eV $< m_{\bar{\nu}_e} <$ 46 eV with 90% CF. Their '83 result from the same experiment obtained now with much improved apparatus is $m >$ 20 eV. There are a number of experiments in progress (Table I) which aim to verify this result.

The most accurate muon neutrino mass measurements were performed by studying the pion decay at rest [5] or in flight and from $K\pi_3$ [6] decays. Experiments to improve the present "best" limit for $m_{\nu_\mu} <$ 490 keV with 90% CL are considered [7–9]. The ν_τ mass was measured by DELCO and MARK I collaborations at SLAC [3, 10]. Another type of experiment which can measure the ν_e mass use the electron capture process [11–13] $Z_{cap} \rightarrow (Z-1)+\nu_e+\gamma$. In this type of measurement some systematic errors present in the tritium experiments can be avoided. Shrock [14] and others suggested that a search for secondary peaks in the lepton momenta spectra of pion and kaon decays can provide sensitive limits for neutrino masses and mixings. In a two body decay each eigenstate would be visible in the lepton recoil spectrum with intensity proportional to the mixing matrix $|U_{1i}|^2$. In the three body decays the existence of neutrino mass will result in cusps or kinks in the decay lepton spectra. The limits for heavy neutrinos coupled to electron neutrinos from nuclear beta decays as a function of $|U_{1i}|^2$ is shown in Fig. 1. For the neutrino mass above 1 MeV the two body decays yield a most stringent limit in the region up to 200 MeV. Similar limits were derived from the muon decay data covering the mass region 20 to 70 MeV (Fig. 2). Searches for heavy neutrinos were conducted in neutrino beams. The established limits by Gronau [20] are

$$310 < M_h < 370 \text{ MeV} \quad \text{for} \quad |U_{\mu h}|^2 < 10^{-6},$$
$$160 < M_h < 480 \text{ MeV} \qquad\quad |U_{eh}|^2 < 10^{-6}-10^{-5}.$$

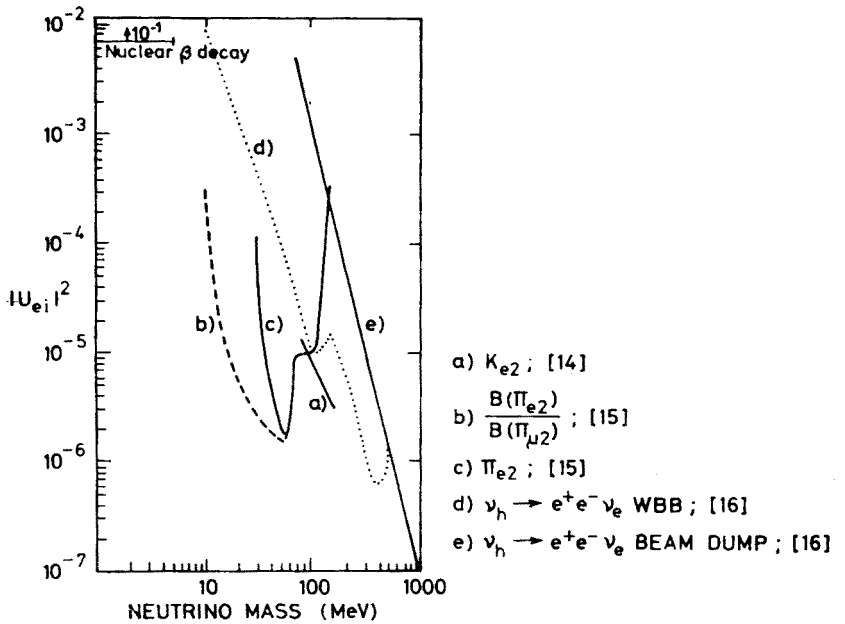

Fig. 1. Limits on the masses of heavy neutrino coupled to electron neutrinos

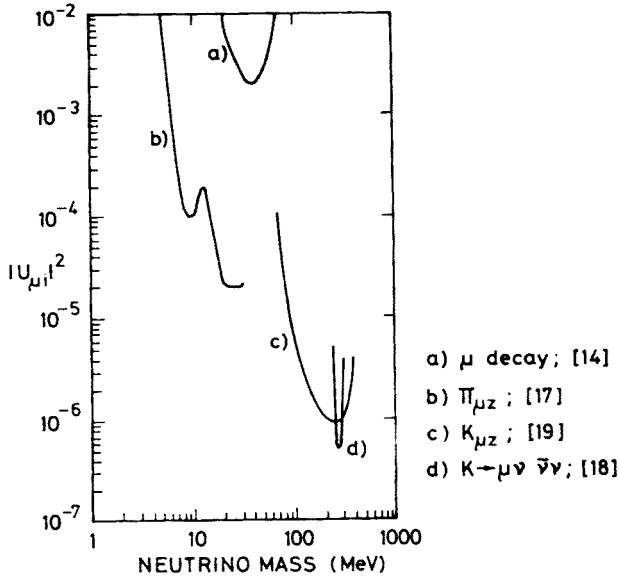

Fig. 2. Limits on the masses of heavy neutrinos coupled to muon neutrinos

The limits on the neutrino masses can be derived from the big-bang nucleo synthesis which limits the number of neutrino flavors to $N_\nu \leqslant 4$ and sets the mass constraints from the rate of the expansion of the universe. The sum of the masses of stable neutrinos must be $10\,\text{eV} < \Sigma m_\nu < 100\,\text{eV}$ [21–23].

Searches for nuclear beta decay yield limits on only Majorana type neutrinos $(\bar{\nu} = \nu)\,(AZ) \to (A, Z+2) + e^- + e^-$. To allow for this forbidden decay by the lepton number conservation the neutrino must have right handed couplings or have mass. The observed limits on the neutrinoless double beta decays can set the limits on the Majorana neutrino masses and their right handed couplings. The existing limits [24] are given in Table II. The double beta decay experiments place a limit on the neutrino mass $m_\nu < 3$–$10\,\text{eV}$. Comparing this limit to the ITEP limit of $\bar{\nu}_e > 20\,\text{MeV}$ implies that the neutrino is a Dirac particle rather than the Majorana type.

At present there are several experiments in progress to improve the above quoted limits.

TABLE II

Source	Half life limit for $0\#\nu$ decay	m_ν limit ($\eta = 0$)	RHC limit ($m_\nu = 0$)	Ref.
^{48}Ca	$> 10^{21.3}$ years	$< 30\,\text{eV}$	—	[25]
^{76}Ge	$> 10^{21.7}$ years	$< 15\,\text{eV}$	$\eta < 3\times10^{-5}$	[26]
^{82}Se	$> 10^{21.5}$ years	$< 12\,\text{eV}$	$\eta < 1\times10^{-5}$	[27]
$^{76}Ge^{76}$	$> 10^{22}$ years	$< 9\,\text{eV}$	$\eta \sim 10^{-5}$	[28]

The firm evidence for the existence of the neutrino mass would have a major impact on the existing GUTS and astrophysical models.

The aim of this paper is to discuss another method for searches for neutrino masses — via the detection of neutrino oscillations. Especially an experiment in progress at LAMPF meson facility at Los Alamos, E-645, will be described.

The interesting possibility of neutrino oscillations was first suggested by Pontecorvo [30]. Analogous to oscillations between K^0 and $\overline{K}^0$ states, neutrinos of one type may transform into another type while propagating through vacuum. This happens if the physical neutrinos are not pure quantum mechanical states, but rather superpositions of mass eigenstates. The oscillation amplitude depends on the magnitude of the mixing strength while the wavelength of the oscillation is determined by the difference in the squares of the mass eigenvalues.

Neutrino oscillations, if experimentally observed, would thus lead immediately to at least two conclusions: (*i*) that the mass of at least one of the neutrino types in non-zero, and (*ii*) that a given lepton number is not separately conserved.

Consider for simplicity oscillations involving only two types of neutrinos, e.g., ν_e and ν_μ. Starting from a pure ν_e beam of energy E, (in MeV), the probability of finding ν_μ in a detector located at distance L (in meters) from the source given by

$$P(\nu_e \to \nu_\mu) = \sin^2(2\theta) \sin^2\left(1.27 \frac{L}{E} \Delta m^2\right), \tag{1}$$

and for the case where $\nu_e \to \nu_e$

$$P(\nu_e \to \nu_e) = 1 - \sin^2(2\theta) \sin^2\left(1.27 \frac{L}{E} \Delta m^2\right), \tag{2}$$

where $\Delta m^2 = M_1^2 - M_2^2$ in eV^2 is the difference of the squares of the neutrino mass eigenstates ν_1 and ν_2, and θ is the mixing angle between them. ν_e, ν_μ may then be represented as

$$\begin{Bmatrix} \nu_e \\ \nu_\mu \end{Bmatrix} = \begin{Bmatrix} \cos\theta & \sin\theta \\ -\sin\theta & \cos\theta \end{Bmatrix} \begin{Bmatrix} \nu_1 \\ \nu_2 \end{Bmatrix}. \tag{3}$$

The oscillation wavelength in meters can be written in view of Eq. (1) as

$$\Lambda = \frac{2.5\,E}{\Delta m^2}.$$

In Fig. 3, we plot contours of constant Δm^2 in the $\Lambda - E$ space. The ranges of sensitivity to neutrino oscillations that can be attained at existing laboratories are also shown. These ranges are estimated on the basis of accessible ν energies and feasible detector to source distances dictated by expected signal-to-noise ratios. We note that the intense low energy neutrino beam at LANL is superior for sensitive neutrino oscillation experiments when compared in this way to the other accelerator facilities in the world.

Experimentally, there exist at least two flavors of neutrinos: ν_e and ν_μ. In addition, the existence of a third flavor neutrino, ν_τ, is inferred from the observation of the $\tau^\pm$ lepton.

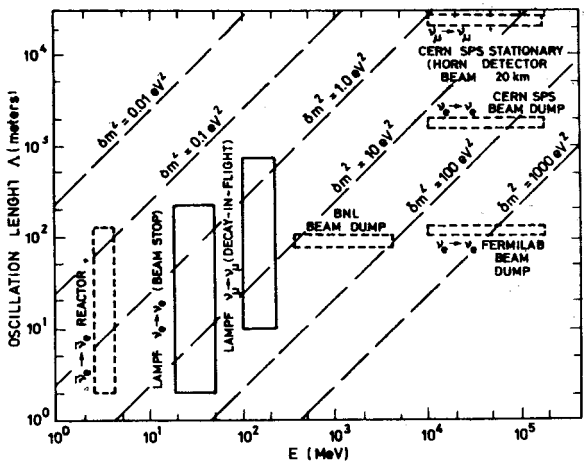

Fig. 3. Contours of constant Δm^2 in the A-E space

Taking into account the three antineutrinos, the possible channels for flavor oscillations to occur are

$$\nu_e \rightleftarrows \nu_\mu;\ \bar{\nu}_e \rightleftarrows \bar{\nu}_\mu,$$

$$\nu_e \rightleftarrows \nu_\tau;\ \bar{\nu}_e \rightleftarrows \bar{\nu}_\tau,$$

$$\nu_\mu \rightleftarrows \nu_\tau;\ \bar{\nu}_\mu \rightleftarrows \bar{\nu}_\tau.$$

It is also possible to have oscillations of the type $\nu_i \rightleftarrows \bar{\nu}_i$ (Majorana neutrino).

Two general classes of experiments can be done:

(*i*) Exclusive experiments in which the probabilities $P(\nu_i \rightleftarrows \nu_j)$ are measured often called appearance experiments.

(*ii*) Inclusive experiments (often referred to as disappearance experiments) in which the probabilities $P(\nu_i \rightleftarrows \nu_i)$ are measured. We note that inclusive experiments are more general since they are sensitive to ν_i oscillating into any other type.

In the exclusive or the appearance experiment the measured limit of $P(\nu_i \leftrightarrows \nu_j)$ can be expressed by a curve in two parameter space defined by $\sin^2(2\theta)$ and Δm^2 using the expression (1). This region is bracketed by the limits as follows:

Small Δm^2 and $\quad (L \ll L_{osc} = 2.5\, E_\nu/\Delta m^2)$.

Large $\sin^2(2\theta) \sim 1$ $\quad \Delta m^2 < P(\nu_i - \nu_j)^{1/2}/1.27 L/E_\nu$.

Large Δm^2 $\quad (L \gg L_{osc}),\ \sin^2(2\theta) < 2P(\nu_i - \nu_j)$.

The sensitivity of an experiment is determined by the background rate of ν_j's, the measured rate of ν_j's, and the value of L/E_ν. Large L/E_ν values give the smallest Δm^2 limits but may decrease the $\sin^2(2\theta)$ sensitivity because the observed ν_i event rate falls with increasing L or decreasing E_ν. In the inclusive or disappearance experiment the flux of given type of neutrinos is measured as a function of distance and energy and the disappearance of

neutrinos as is given by (2). The Δm^2 sensitivity in this type of experiments is limited by the statistical and systematic errors also. In this type of experiments in order to minimize the systematic errors two detectors should be used running simultaneously and located at two distances in a neutrino beam. A high limit on Δm^2 sensitivity is achieved when the distance between the neutrino source and the detector is many oscillation lengths away and is reached when the following conditions are met:

$$L_{\text{source}} < L_{\text{oscillations}} = \frac{2.5\, E_\nu}{\Delta m^2}$$

and the energy resolution for the detected ν events is

$$\frac{\Delta E_\nu}{E_\nu} < \frac{0.2}{\text{Number of oscillation length in } (L_S - L_D)},$$

$L_S - L_D$ – distance between ν source and detector.

There is no fundamental upper limit for Δm^2 if the size of the neutrino source and the neutrino flux and spectrum are known.

The disappearance experiments can be performed at high power reactors and accelerators. At the accelerators where only pions and muons are produced the flavor and the intensity of the neutrino beams are well known.

In the past there were several experiments yielding results which could be interpreted in terms of neutrino oscillations. The reactor experiment at the Le Bugey reactor may have observed oscillations and a possible mass difference of $\Delta m^2 = 0.20\ \text{eV}^2$ for $\sin^2(2\theta) = 0.25$ has been reported. Also, the results on the detected ratios of ν_e/ν_μ prompt events in several beam dump events allow for the possibility of ν oscillations. The limits are shown below:

$$\text{Ratio } \frac{\nu_e \text{ events}}{\nu_\mu \text{ events}} = 1.09 \pm 0.09 \pm 0.10 \quad \text{Fermilab (E613)}$$

$$0.83 \pm 0.13 \pm 0.12 \quad \text{CDHS}$$

$$1.35^{+0.65}_{-0.35} \quad \text{BEBC}$$

$$0.59 \pm 0.11 \pm 0.08 \quad \text{CHARM}$$

No strong conclusion can be drawn from these results and the large range of measured values precludes any definitive statements about the presence of absence of neutrino oscillations. The experiment measuring the solar neutrino flux observes a large discrepancy in the measured and calculated flux of neutrinos. The measured flux [29] is 2.1 ± 0.3 SNU (1SNU = 10^{-36} ν captured per second in Cl^{37} atom) and the rate predicted from standard solar calculation [31, 32] is in the range of 5.2 ± 2.0 and 7.9 ± 1.9 SNU. Finally the meson results of the cosmic neutrino rates and its comparison to the calculated spectrum [33–35] is:

$$\frac{\nu_\mu \text{ flux observed}}{\nu_\mu \text{ flux calculated}} = 0.98 \pm 0.20$$

which leaves a possibility for ν oscillations.

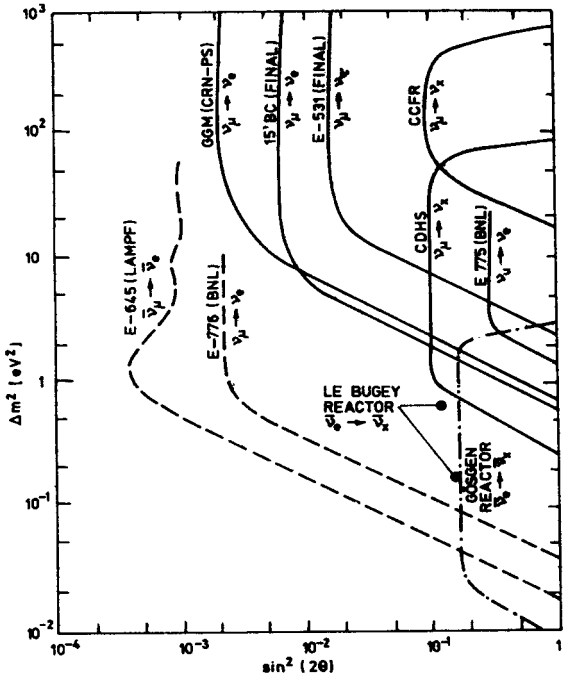

Fig. 4. Sensitivity plots

TABLE III

Existing neutrino oscillation limits

	$\nu_\mu \to \nu_x$		$\nu_\mu \to \nu_e$		$\bar{\nu}_e \to \bar{\nu}_x$		
	Δm^2	$\sin^2(2\theta)$	Δm^2	$\sin^2(2\theta)$	Δm^2	$\sin^2(2\theta)$	Notes
CHARM [36]	0.3	0.2	0.2	0.05			—
CDHS [37]	0.25	0.05					"best fit" $\Delta^2 = 0.32$, $l^2 = 0.2$
BNL [38]			10	0.005			—
FNAL [39]	1	0.05					room for osc. in large Δ^2
Goesgen [40]					10^{-2}	0.15	small s^2 $\Delta^2 = 500$, $s^2 = 0.06$
Le Bugey [41]					0.1	0.10	high statistics hint at $\Delta^2 = 0.6$, $s^2 = 0.1$
Beam Dump [42]							$\nu_e \to \nu_\tau$ with $\Delta_2 = 360 \pm 40$ $s^2 = 0.32^{+0.18}_{-0.08}$

TABLE IV

Upcoming exclusive oscillation experiments

		Large Δm^2 $\sin^2(2\theta)$ limit	$\sin^2(2\theta) = 1$ Δm^2 limit
BEBC ($\nu_\mu \to \nu_e$)	Low energy horn $\langle E_\nu \rangle \approx 1$ GeV	5×10^{-3}	0.04 eV^2
BNL E776 ($\nu_\mu \to \nu_e$)	NBB $\langle E_\nu \rangle \approx 1.5$ GeV	1×10^{-3}	0.03 eV^2
BNL E775 ($\nu_\mu \to \nu_e$)	NBB $\langle E_\nu \rangle \approx 1.5$ GeV	1×10^{-3}	0.2 eV^2
LAMPF E645 ($\bar{\nu}_\mu \to \bar{\nu}_e$)	Beam stop beam $\langle E_\nu \rangle \approx$ 0–53 MeV	8×10^{-4}	0.05 eV^2
Old limits		6×10^{-3}	0.06 eV^2

TABLE V

Upcoming inclusive experiments

Accelerator experiments	Source	Sensitivity	
		Δm^2 Range	Best $\sin^2(2\theta)$
CHARM $\nu_\mu \to \nu_x$	Low E are largest	0.3–7 eV^2	$0.02/\Delta m^2 = 2$ eV^2
BNL E776 $\nu_\mu \to \nu_x$	NBB $\langle E_\nu \rangle = 1.5$ GeV	0.13–100 eV^2	$0.02/\Delta m^2 = 2$ eV^2
BNL E775 $\nu_\mu \to \nu_x$	WBB $\langle E_\nu \rangle = 2$ GeV	5–100 eV^2	$0.2/\Delta m^2 = 25$ eV^2
	NBB $\langle 1.5$ GeV$\rangle$	0.2–100 eV^2	$0.03/\Delta m^2 = 1$ eV^2
LAMPF E645 $\nu_e \to \nu_x$	Beam stop beam	0.2–25 eV^2	$0.10/\Delta m^2 = 10$ eV^2

Reactor experiments ($\bar{\nu}_e \to \bar{\nu}_x$)		Sensitivity $\Delta m^2 = 0.02$–10 eV; $\sin^2(2\theta) > 0.1$	
		Position	Count rate
Bugey		13.5 m	26 counts/hr
Annecy-ISN-Grenoble)		17.5 m	16
Savannah River		17.5 m	20
(UCI)		24 m	11
Goesgen	done	37.9 m	3.2
	done	45.7 m	2.2
	new	65 m	1.1

There were several experiments in the past which searched for neutrino oscillations. The summary of achieved limits on Δm^2 and $\sin^2(2\theta)$ is shown in Table III and Fig. 4. The searches for neutrino oscillations planned for the near future are listed in Tables IV and V.

E-645 search for ν oscillations at LAMPF, Los Alamos National Laboratory

This experiment is a collaboration between Argonne National Laboratory, California Institute of Technology, Louisiana State University, Los Alamos Laboratory and The Ohio State University (Fig. 5).

E-645 COLLABORATION

Argonne National Laboratory —

S. Friedman, M. Green, K. Leskol, J. Napolitano

California Institute of Technology —

R. D. McKeown, B. Fujikawa

Louisiana State University —

R. Imlay, W. J. Metcalf, A. Fazeley, C. Choi

Los Alamos —

J. Donahue, J. Garvey

The Ohio State University —

T. Y. Ling, J. Mitchell, T. A. Romanowski, E. Smith, M. Timko

Fig. 5

The Los Alamos meson facility is an excellent source of neutrinos. The neutrino beam is produced in a beam dump by 1 ma current of protons with 800 MeV kinetic energy. The neutrino flux at the source is 3×10^9 cm^{-2} sec^{-1} and is essentially a pure ν_e, ν_μ and $\bar{\nu}_\mu$ beam dump produced by stopping π^+ and μ^+ (π^-, μ^- are absorbed in the beam dump). The energy of the ν is in the range $0 < E_\nu < 53$ MeV, (Fig. 6).

The aim of the experiment is to search for neutrino oscillations in two different channels: (*i*) the appearance of $\bar{\nu}_e$ via the detection of $\bar{\nu}_e + p \rightarrow e^+ + n$ and (*ii*) the disappearance of ν_e by measuring the energy and distance dependences of the rate of $\nu_e + d \rightarrow e^- + p + n$. These experiments will achieve sensitivities in Δm^2 ranging from 0.01 eV^2 to 20 eV^2 and $\sin^2(2\theta)$ down to 0.001.

The detector, shown in Fig. 7, consists of planes of active elements in the form of scintillation or Cherenkov counters and planes of proportional drift tubes (PDT). The counters, made of acrylic extrusions of dimension $144'' \times 12'' \times 1.3''$, can be filled with D_2O, H_2O or liquid scintillator to serve as targets for neutrino interactions. Signals generated in these counters are used to trigger the detector and to identify the electrons. The

PDT planes are interspaced throughout the detector for tracking and to provide additional dE/dx measurement of the electrons. The counters and PDT's together yield enough redundancy for electron identification and energy measurement of the observed event. The total mass of the active part of the detector is about 20 metric tons.

In order to shield against beam associated and cosmic ray backgrounds, the detector is surrounded on all sides by 7 inches of lead to absorb incoming photons and 6 inches of liquid scintillator to veto charged particles with high efficiency. The detector and the shield together will be housed in an underground tunnel with 2500 g/cm^2 of earth overburden for protection against cosmic ray or beam-related neutrons (Fig. 8).

In the disappearance experiment the detector will be split into two parts; a 5 ton module remaining stationary and a 15 ton movable module which will permit the search

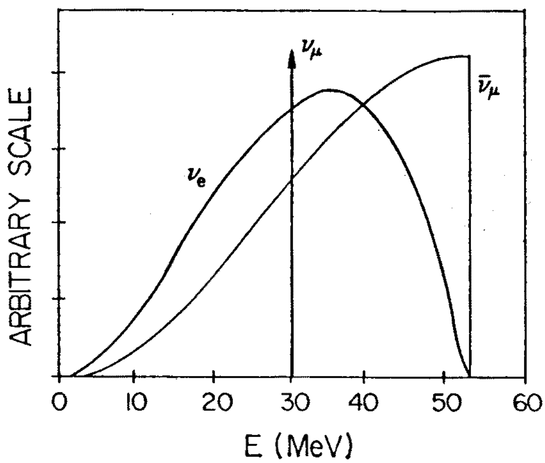

Fig. 6. Neutrino spectra from beam stop $\pi^+ \rightarrow \mu^+ + \nu_\mu$
$\quad\quad\quad\quad\quad\quad\quad\quad\quad\quad\quad\quad\quad\quad \hookrightarrow e^+ + \nu_e + \bar{\nu}_\mu$

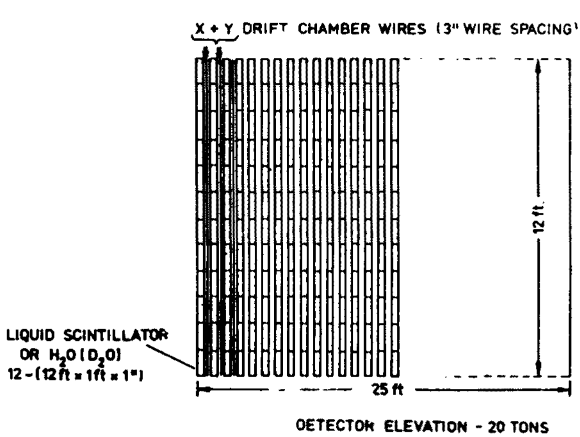

Fig. 7. Detector

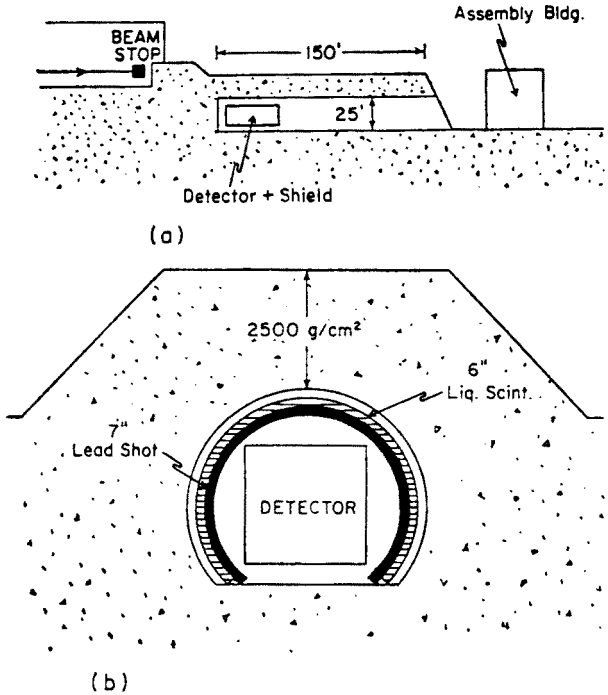

Fig. 8. a) Side view of E645 tunnel, b) Cross section of tunnel and cosmic ray shield of E645

in a flux independent way and provide the capability to demonstrate spatial oscillations should a positive signal be observed.

Characteristics of the detector are:

(1) 20 tons of active target-liquid scintillator or D_2O,
(2) x and y particle tracking with proportional drift tubes (PDT),
(3) measurement of dE/dx in scintillators and PDT's,
(4) total visible energy measurement by particle range and scintillator counter response,
(5) neutron detection,
(6) event trigger with time windows in the past for 50 μs and the future for 100 μs and correlation with active shield,
(7) fine granularity ΔE 6 MeV/module for minimum ionizing particles,
(8) aluminium free detector,
(9) active and passive cosmic ray shield.

Construction of the PDT

The PDT cells are made of laminated Kraft paper helically wound to form 144″ long tubes with rectangular cross section 1.5″ × 3″. The inner wall of the tube is an overlapped layer of aluminum mylar adhesive tape. The thickness of aluminum on the tape is 1 mm and the thickness of the laminated Kraft paper is 60 mm (0.11 g/cm²). Figure 9 shows a cross sectional view of the tube.

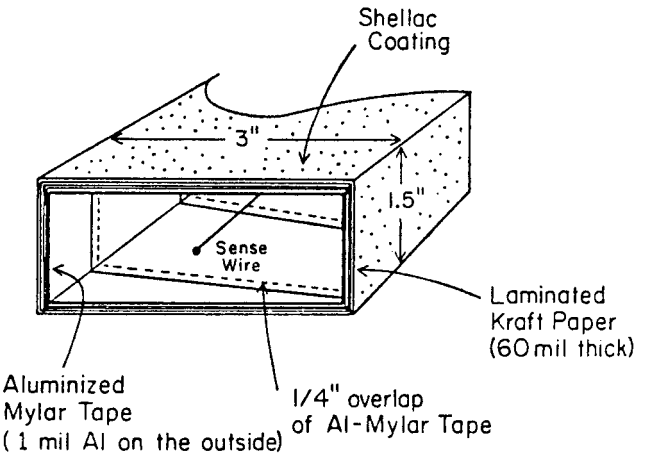

Fig. 9

Performance of the prototype PDT

The prototype PDT was extensively tested with cosmic rays. The gas used for the PDT was 90% argon and 10% methane mixture at sea-level atmospheric pressure. The efficiency of the PDT under this operating condition is plotted versus high voltage on the sense wire and is shown in Fig. 10. The PDT cell can be operated in the proportional drift mode within an interval of 200 volts centered aroung 2.3 kV.

The drift time measured is plotted against drift distance for each cosmic ray track, shown in Fig. 11. The performance of the paper chamber was found to be very similar to that of a chamber of the same size made of 20 mm thick aluminum walls. The solid curve shown in Fig. 11 is the result of a calculation involving electric field mapping. The agreement between the calculation and both sets of data is very good. Position resolution of 1 mm is achieved.

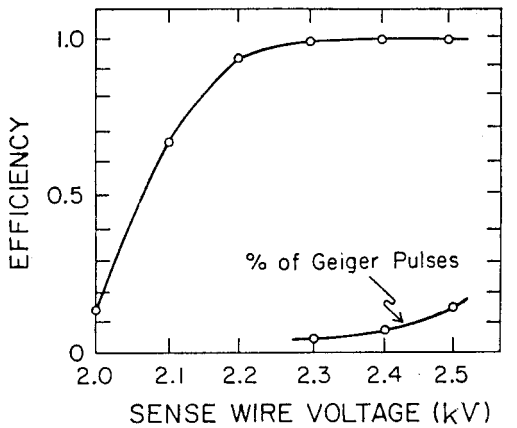

Fig. 10. The efficiency of the PDT cell as a function of sense wire voltage

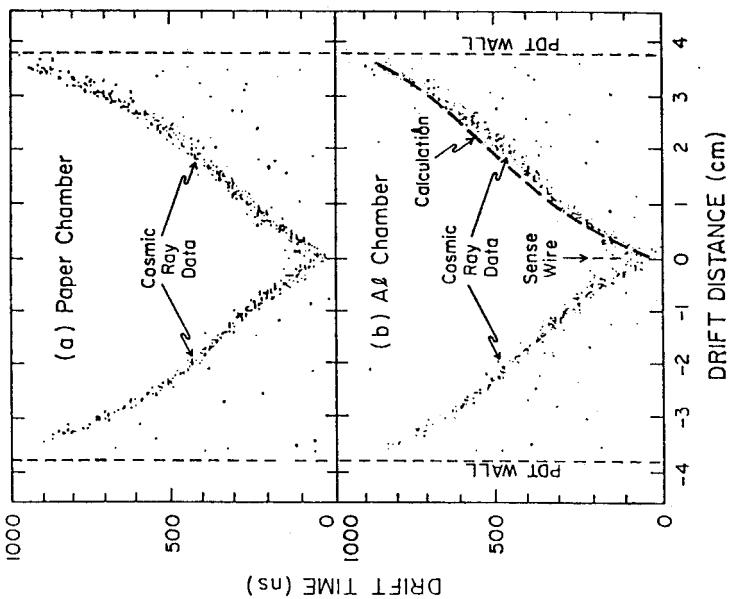

Fig. 11

Fig. 11. Scatter plot of drift time versus drift distance obtained with cosmic ray tracks for a) — a PDT cell made of Kraft paper lamination, b) — a PDT cell of the same size made of 20 mm thick aluminum. The dashed curve is the result of a calculation taking into account the shape of the electric field and the dependence of drift velocity of electrons on the electric field

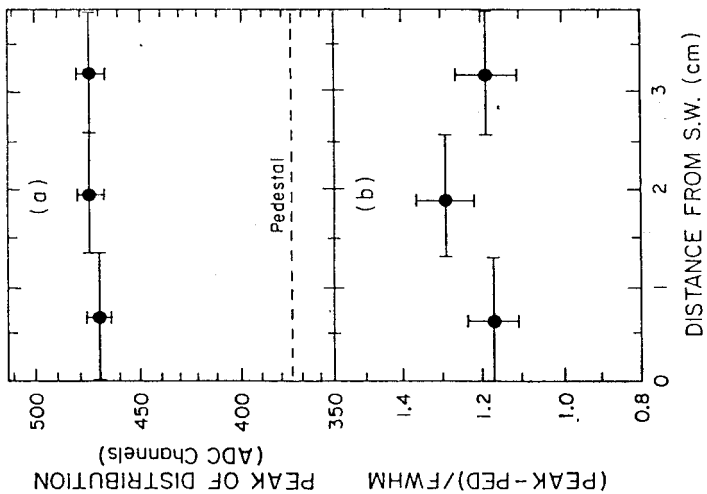

Fig. 12

Fig. 12. a) The peak of charge distribution plotted against the distance of tracks from the sense wire, b) the ratio (peak/FWHM) of the charge distribution plotted against track distance from the sense wire

The peak of the charge distribution plotted against drift distance shown in Fig. 12a indicates charge uniformity over the entire cell. The ratio of peak position to full width at half-maximum of the charge distribution is also observed to be uniform over the whole cell as shown in Fig. 12b. The average value of the ratio measured is 1.2, corresponding to 35% resolution of the measured ionization energy deposited by the traversing charged particle.

Liquid scintillator/Cherenkov counters

The 12 ft long lucite extrusions are viewed on each end with a photomultiplier (Hamamatsu R878). One response from these counters was measured using the minimum ionizing cosmic ray muons and is shown in Fig. 13.

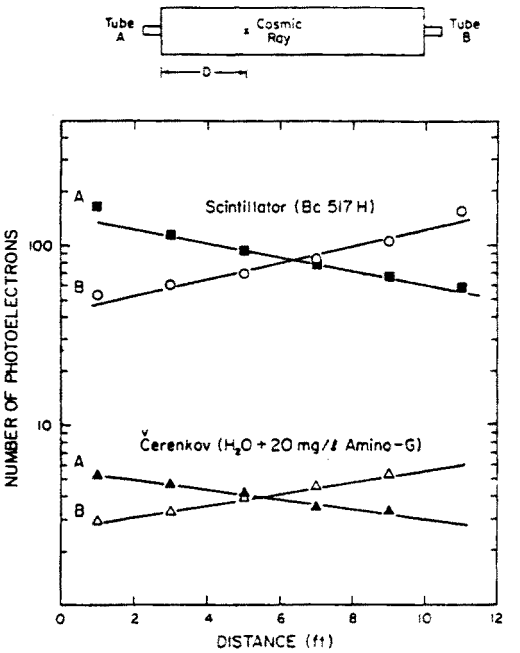

Fig. 13. Scintillation/Cherenkov counter response

Electronic trigger and digitization

The fast event trigger with a time resolution of 150 ns will require an interaction anywhere in the detector caused by a neutral particle. This trigger also requires a veto signal from the cosmic ray shield, furthermore, in order to assure that a minimum energy is deposited by the event a "hit" with at least 2 or 3 consecutive planes will be demanded. The total energy of the event is in the range of $20 < E < 53$ MeV. The pulses from the scintillation counters and drift tubes will be digitized in height and time. The past (40 ns) and future (100 ns) history of the detector will be recorded around the event trigger. This technique will enable for better rejection of background caused by stopping muons and allow for the detection of neutrinos.

Neutron detection

The detection of neutrons is achieved by capture $\sigma_c = 5 \times 10^4$ baryons in a layer of Gadolinium 10 gm/cm^2 thick deposited on paper sheets placed between the scintillation and drift chamber planes. The neutron capture is accompanied by emission of up to 4γ rays with total energy of 8 MeV and the thermalization time for the neutrons is 100 μs. The resulting γ rays from capture will be detected in the scintillation counters.

The active and passive shield

The detector is nested in the active and passive shield which is to provide a veto signal for passing charged particles and also to attenuate the γ rays produced by the cosmic rays in the overburden. The cosmic ray flux incident on the detector is 10 kHz. The electrons from stopping muons in the shielding surrounding the tunnel are sources of γ's which if was absorbed can make a neutrino like event. Also the neutrons from the muon captures in the overburden can originate γ rays. The shield is viewed by 340 photomultipliers and the response will be recorded and correlated with the event trigger. The estimated sources of backgrounds in this experiment are shown in Table VI. Tests of the prototype of the shield showed that a rejection ratio for expected backgrounds in the range of 10^{16} is achievable. Our overall aim is to keep the neutrino like backgrounds to 0.1/day.

TABLE VI

Background estimates table
E645 shield — summary sheet

Cosmic radiation	Flux at LAMPF (cm^{-2} sec^{-1})	Overburden (2500 g/cm^2) attenuation	Active shield rejection	Passive shield attenuation	Detector rate LD^{-1}
$\mu^{\pm}$	1.93×10^{-2} (4.3% stop)	0.23	$< 10^{-7}$	—	$< 6.5 \times 10^{-2}$
$n(E > 65$ MeV)	2.2×10^{-3}	3.7×10^{-6}	—	0.4	4.5
$\mu^{\pm}$ (brem)	1.1×10^{-7}	—	$\ll 1$	3×10^{-6}	$< 4.6 \times 10^{-4}$
$\mu^+ \rightarrow e^+$ (brem)	1.1×10^{-7}	—	—	3×10^{-6}	2.2×10^{-3}
$\mu^- + N \rightarrow n + X$	8.3×10^{-8}	—	-76	0.135	29

Act. shield: 15 cm of liq. scint.; passive shield: 5.1 cm Fe+12.7 cm Pb; active shield rejection $\equiv 1 - \frac{N_{\text{det.}}}{N_{\text{inc.}}}$

LAMPF day = 5.2×10^3 sec; area top = 0.26×10^6 cm$^2 \times$ LD = 1.4×10^9 cm^2 sec; Σ area = 1.3×10^6 cm$^2 \times$ LD = 6.8×10^9 cm^2 sec; detector mass = 1.8×10^7 grams; overburden: $\frac{2500\ \text{g}}{\text{cm}^2}$ gravel.

Data acquisition system

The data will be acquired on-line by a PDP 11/23 computer linked to a VAX 11/750 for event processing.

The PDP 11/23 will also process on-line tests and monitor the detector.

Tests of the prototype detector

In order to learn about the event identification and energy resolution and the background rejection of the detector, we have measured the response of a prototype of the E-645 detector to incident positrons and protons in the LAMPF test beam. The apparatus consisted of ten layers, each with two scintillator tanks stacked vertically and a set of 9 vertical and 9 horizontal proportional drift tubes (PDT's) (Fig. 14). The area subtended by the detector perpendicular to the beam was 3′ wide and 2′ high. The ten planes corresponded to a total depth of 45 g/cm^2. Beam particles incident were selected by the time-of--flight and a clear separation between electrons, pions and protons was achieved.

The energy response of the detector was calibrated by using the most probable energy deposition per counter of 500 MeV/c muons (nep). The response to muons was recorded periodically to avoid systematic drifts of the system. A typical response of liquid scintillator counters to muon energy loss is shown in Fig. 15. The performance of the detector to

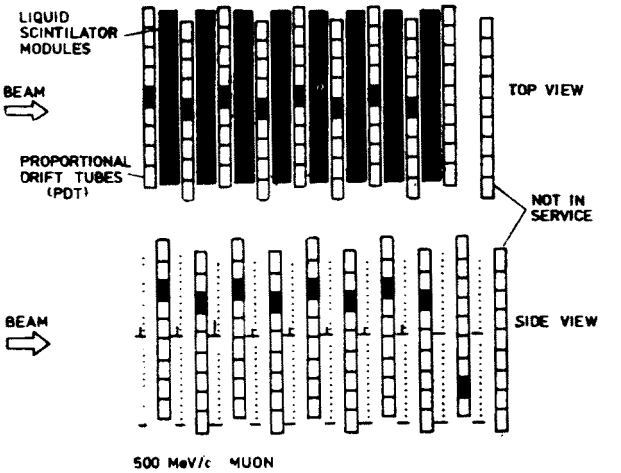

Fig. 14. Prototype detector-test

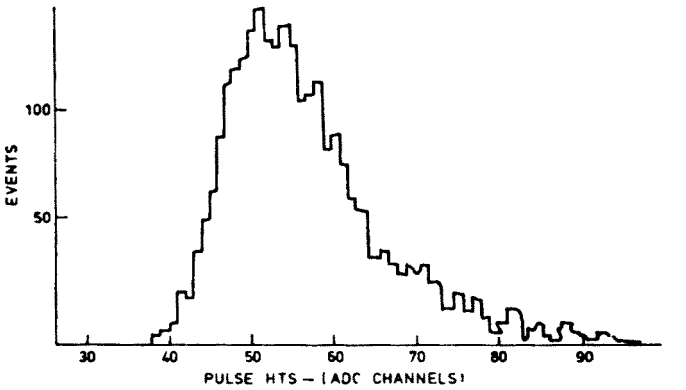

Fig. 15. Muon energy deposition (500 MeV/c) in one scintillation ctr. module

particles incident at angles other than normal was also investigated (30° and 45°). The visible energy distribution for detected electrons at 0° incidence angle in the energy region 60, 50 and 40 Me/c are shown in Fig. 16 and in Fig. 17 we have plotted the peak of the electron energy distribution as a function of the nominal beam settings. Radiation losses are important, therefore we show two estimates which relate the visible to the total electron energy; in one we assume that the energy lost through both ionization and radiation is de-

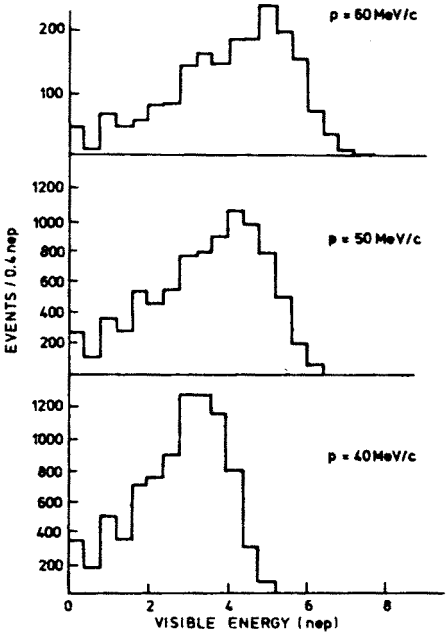

Fig. 16

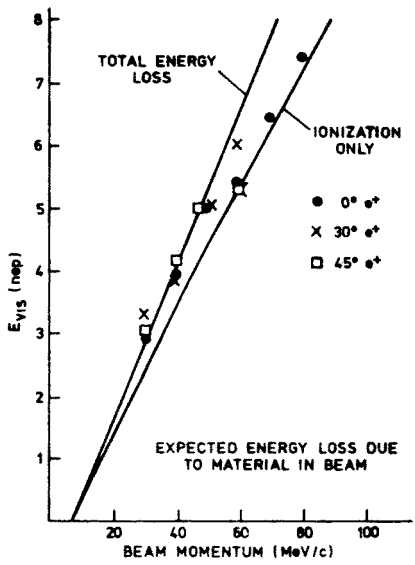

Fig. 17

Fig. 16. Positron beam normal incident visible energy loss for electrons
Fig. 17. Energy loss by e^+ in detector

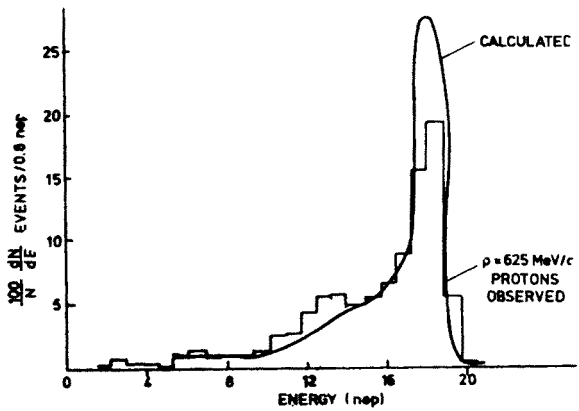

Fig. 18. Visible energy calculated and observed, normal incidence

tected in the other that only collision losses are observed. The calculated visible energy excludes the energy lost downstream of the first module with less than 0.2 nep. Thus, we expect that the visible energy would correspond more closely to the curve which represents ionization losses only. The visible energy loss by electrons was compared with a Monte Carlo calculation and both distributions were found to be in good agreement.

The fraction of energy deposited by protons in the live region of the detector depends largely on where the particle ranges. If the proton ends its range in the dead material, up to 30% of its energy will be invisible. Anywhere from 20 to 40% of the proton energy can be lost in the dead space. To understand the energy lost by incident protons in the test detector, it was necessary to determine the location of the dead spaces along the particle's trajectory. This was done at two beam settings which were calibrated by range: $P = 625$ MeV/c corresponded to $T = 178$ MeV and $P = 500$ MeV/c was found to have particles with $T = 121$ MeV. Using the measured kinetic energy distributions as input to an energy loss program, we have been able to reproduce the two energy distributions quite well (Fig. 18).

Electron-proton identification

The experiment E-645 uses the positron from $\bar{\nu}_e + p \rightarrow e^- + n$ to identify the charged current interaction. Therefore it is important to be able to reject all backgrounds which produce a single charged track. Protons, produced by incoming neutrons, are identified by their high ionization toward the end of their range.

Estimates of the neutron flux in the detector (200/LANL day) demand that the detector be able to reject protons by a factor of 200 to 1 to keep the background levels at 0.1 per LAMPF day.

For charged particles of a fixed range, protons will deposit more energy. Thus, different particles appear as stripes on a total visible energy vs. range plot (Fig. 19). The vertical

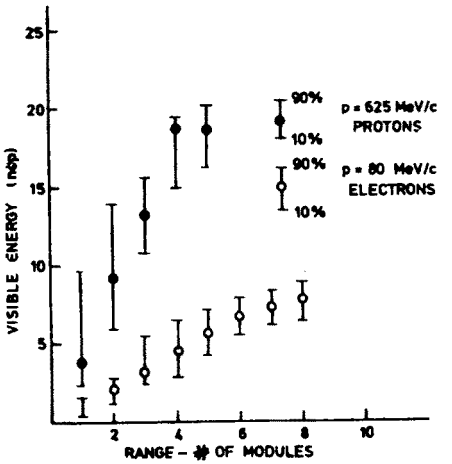

Fig. 19. Total visible energy for e+p vs range

lines on the plot show the region of energy which contain 80% of the data. The actual proton rejection and electron efficiency can be read off energy histograms at fixed range (Fig. 20).

For particles with a range of two planes and $E < 5.6$ nep, 5% electrons are eliminated and 4% of the protons are kept. For particles with a range of three planes, we eliminate $\sim 1\%$ of the electrons and keep the same fraction of protons. Practically all protons with a larger range (> 3 planes) can be eliminated with the electron sample not suffering any significant reduction (Fig. 20). Pulse heights in the PDT's provide an independent and

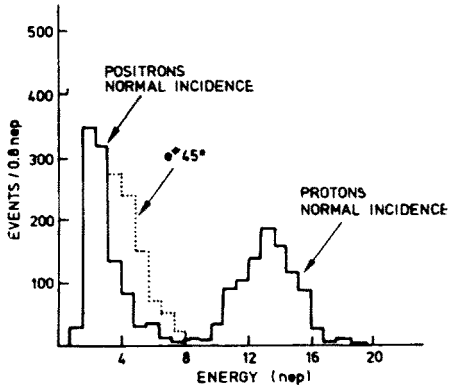

Fig. 20. Energy loss for positrons and protons with fixed range of 3 modules

additional cuts for the discrimination between protons and electrons. It appears that the rejection of protons from electrons can be achieved at the level of 10^4 with little loss of electrons. Assembly of the detector is now in progress and we expect to take data in April of 1985.

Editorial note. This article was proofread by the editors only, not by the author.

REFERENCES

[1] V. A. Lubimov, Proceedings of the European Physical Society HEP 83, Brighton, England 1983.
[2] R. Abela et al., *SIN Newsletter* **15**, p. 26.
[3] C. Matteuzzi et al., *Phys. Rev. Lett.* **52**, 1869 (1984).
[4] V. A. Lubimov et al., *Phys. Lett.* **94B**, 266 (1980).
[5] D. C. Lu et al., *Phys. Rev. Lett.* **45**, 1066 (1980).
[6] A. R. Clark et al., *Phys. Rev.* **D9**, 533 (1974).
[7] P. Seller, *Neutrino Mass and Gauge Structure of Weak Interactions*, Telemark, Wisconsin 1982, p. 41.
[8] B. Robinson, *Neutrino Mass and Gauge Structure of Weak Interactions*, Telemark, Wisconsin 1982, p. 25.
[9] C. Hoffmann, V. Sandberg, Proceedings of the 1982 DPF Summer Study, Snowmass, Colorado, p. 552.
[10] W. Bacino et al., *Phys. Rev. Lett.* **42**, 749 (1979).

[11] C. L. Bennett et al., *Phys. Lett.* **107B**, 19 (1981).
[12] A. DeRujula, *Nucl. Phys.* **188B**, 414 (1981).
[13] J. U. Andersen et al., *Phys. Lett.* **113B**, 72 (1982).
[14] R. Shrock, *Phys. Lett.* **96B**, 159 (1980); *Phys. Rev.*
[15] D. A. Bryman et al., *Phys. Rev. Lett.* **50**, 1546 (1983).
[16] F. Bergama et al., CERN-EP/83-63 (Submitted to Phys. Lett.); K. Winter, Proceedings of the Lepton--Photon Symposium, Cornell University 1983.
[17] R. Abela et al., *Phys. Lett.* **105B**, 263 (1981).
[18] C. Y. Pang et al., *Phys. Rev.* **D8**, 1989 (1973).
[19] R. S. Hayano et al., *Phys. Rev. Lett.* **49**, 1305 (1982).
[20] M. Gronau, SLAC-PUB-2967, August 1982.
[21] K. A. Olive, D. N. Schramm, G. Steigman, *Nucl. Phys.* **B180**, 497 (1981).
[22] K. Freese, D. N. Schramm, Fermilab Preprint 83/46-THY, May 1983.
[23] S. Tremane, J. E. Gunn, *Phys. Rev. Lett.* **42**, 407 (1979).
[24] W. C. Haxton et al., *Phys. Rev. Lett.* **47**, 153 (1981); *Phys. Rev.* **D25**, 2360 (1982).
[25] R. Barden et al., *Nucl. Phys.* **A158**, 337 (1970).
[26] E. Fiorini et al., *Nuovo Cimento* **A13**, 747 (1973).
[27] B. T. Cleveland et al., *Phys. Rev. Lett.* **35**, 737 (1975).
[28] E. Bellotti et al., Proceedings of the European Physical Society HEP 83, Brighton, England (1983); E. Bellotti, Neutrino 82, p. 216, Balaton, Hungary 1982.
[29] S. M. Bilenky, B. Pontecorvo, *Phys. Rep.* **41**, 226 (1968).
[30] R. Davis et al., in: Proceedings of the Telemark Neutrino Mass Miniconference, Telemark, Wisconsin 1980.
[31] J. N. Bahcall et al., *Phys. Rev. Lett.* **45**, 945 (1980); J. N. Bahcall, Neutrino 81, Maui, Hawaii 1981.
[32] B. Fillipone, Neutrino 81, Maui, Hawaii 1981.
[33] M. F. Crouch et al., *Phys. Rev.* **D18**, 2239 (1978).
[34] M. M. Boliev et al., Proceedings of the 17th International Cosmic Ray Conference **7**, 106 (1981), Paris, France.
[35] M. R. Krishnaswany et al., report at Neutrino 82, Balaton, Hungary 1982.
[36] J. Blietschau et al., *Nucl. Phys.* **B133**, 205 (1978).
[37] H. J. Meyer et al., Proceedings of the European Physical Society HEP 83, Brighton, England 1983.
[38] N. J. Baker et al., *Phys. Rev. Lett.* **47**, 1576 (1981).
[39] C. Haber et al., Fermilab preprint CONF-83-57-EXP; D. Garfinkle et al., Proceedings XVIII Rencontre de Moriond, (Aim La Plagne, France; March, 1983), U of Rochester preprint UR 853; D. Garfinkle et al., Proceedings of the 11th SLAC Summer Institute of Particle Physics, Stanford, CA, August 1983.
[40] F. Boehm, Proceedings of the Fourth Workshop on Grand Unification, U of Pennsylvania, April, 1983; J. L. Vuillemier, Proceedings of the European Physical Society HEP 83, Brighton, England, July 1983.